LETTERS
PUBLISHED ONLINE: 30 MARCH 2015 | DOI: 10.1038/NPHOTON.2015.42

nature photonics

Continuous-variable entanglement on a chip

Genta Masada[1,2], Kazunori Miyata[1], Alberto Politi[3], Toshikazu Hashimoto[4], Jeremy L. O'Brien[5] and Akira Furusawa[1]*

Encoding quantum information in continuous variables, as the quadrature of electromagnetic fields, is a powerful approach to quantum information science and technology[1]. Continuous-variable entanglement (light beams in Einstein–Podolsky–Rosen, or EPR[2], states) is a key resource for quantum information protocols[3] and enables hybridization between continuous-variable and single-photon discrete-variable qubit systems[4]. However, continuous-variable systems are currently limited by their implementation in free-space optical networks, and the demand for increased complexity, low loss, high-precision alignment and stability, as well as hybridization, require an alternative approach. Here we present an integrated photonic implementation of the key capabilities for continuous-variable quantum technologies—the generation and characterization of EPR beams in a photonic chip. When combined with integrated squeezing and non-Gaussian operations, these results will open the way to universal quantum information processing with light.

The use of quantum-mechanical systems to encode, transmit and manipulate information promises the development of revolutionary technologies in the fields of sensing, computing and communications[5]. There are two natural ways to encode information in the quantum domain: (1) make use of two (or more) discrete levels of a quantum system (for example, the spin of an electron or the polarization of a photon) or (2) use a continuum of states (for example, a quantized harmonic oscillator) that can be described by continuous variables such as the position and momentum of a particle. Light is particularly suited to the encoding of information in the quantum domain and has been successfully used to demonstrate quantum protocols both with discrete variables (DVs) using the degrees of freedom of single photons[6,7] and continuous variables (CVs) using the quadratures of beams of light[8,9].

DV systems benefit from high-fidelity operations, but are currently limited by the imperfect generation and detection of single photons, as well as the absence of deterministic interactions of photons. In contrast, CV schemes can achieve deterministic, unconditional operation, but demonstrate lower fidelities for the majority of quantum protocols. A new hybrid approach overcomes these problems by combining the benefits of DVs and CVs in a single system[4]. Entanglement between DV and CV systems[10,11] and teleportation of a DV state using CV protocols[12] have already been demonstrated. However, practical applications of this hybrid approach will require an integrated system in which light is guided, manipulated and made to interfere in a waveguide architecture. Integrated waveguide circuits have been successfully developed for DV applications[13,14] and have demonstrated high-fidelity and reliable operation. A benefit of this optical integration, in addition to the miniaturization of quantum circuits, is attainment of a high degree of spatial mode matching, which is essential for classical and quantum interference, without any optical adjustment[15]. Transferring CV systems to such integrated circuits presents considerable technical challenges, including achieving high-efficiency coupling, low-loss operation and a high degree of mode matching, all in an architecture that is compatible with DV operation.

Here, we demonstrate an integrated circuit that can be reconfigured to implement the fundamental operations required for CV quantum optics, and which is compatible with high-fidelity DV operation[16]. We characterize a device composed of directional couplers that can interfere two squeezed states of light, perform phase stabilization, and mix strong local oscillator (LO) beams to perform homodyne detection. We further configure the integrated optical circuit to generate and characterize Einstein–Podolsky–Rosen (EPR) entangled beams of light, obtaining a correlation variance of $\Delta^2_{1,2} = 0.71$ that demonstrates inseparability. This shows all the components required to achieve quantum teleportation[8], a Gaussian operation and the most fundamental quantum information protocol, on a single integrated chip.

We first demonstrate that photonic circuits can be used in CV quantum optics and provide the required suppression of coupling between different waveguide modes. Unwanted cross-coupling typically results from stray light arising from insufficient coupling from fibre inputs, waveguide bending losses and cladding guiding. Such cross-coupling is a major limitation in quantum optical networks, reducing the fidelities of quantum operations. It is particularly troublesome for balanced homodyne measurements, because quantum information is encoded on weak optical signals and the presence of light scattered from intense coherent beams such as the LO can degrade the signal and destroy non-classical effects. Here we avoid the harmful consequences of stray light by using the side bands of the optical field and almost perfect mode matching between squeezed light (SL) and LO within a chip, as shown below.

Figure 1 presents the experimental set-up, where the optical network consists of a silica-on-silicon chip that includes four waveguide interferometers (see Supplementary Section I for details). The interferometers are composed of a pair of directional couplers and a phase shifter implemented by a resistive heater lithographically defined on top of one waveguide arm[14]. By tuning the drive current of each resistive heater it is possible to control the optical phase difference between the two arms. Each interferometer is therefore equivalent to a tunable beamsplitter (BS). As shown in Fig. 1a, the squeezed light SL_1 and local oscillator LO_1 are coupled into the chip and superimposed at beamsplitter BS_2. Output beams are collected by optical fibres and measured by a balanced homodyne detector outside the chip. The experiment was performed at a 1.5 MHz side band of the laser frequency.

[1]Department of Applied Physics, School of Engineering, The University of Tokyo, 7-3-1 Hongo, Bunkyo-ku, Tokyo 113-8656, Japan. [2]Quantum ICT Research Institute, Tamagawa University, 6-1-1 Tamagawa Gakuen, Machida, Tokyo 194-8610, Japan. [3]School of Physics and Astronomy, University of Southampton, Southampton SO17 1BJ, UK. [4]NTT Device Technology Laboratories, 3-1, Morinosato, Wakamiya, Atsugi, Kanagawa 243-0198, Japan. [5]Centre for Quantum Photonics, H. H. Wills Physics Laboratory and Department of Electrical and Electronic Engineering, University of Bristol, Merchant Venturers Building, Woodland Road, Bristol BS8 1UB, UK. *e-mail: akiraf@ap.t.u-tokyo.ac.jp

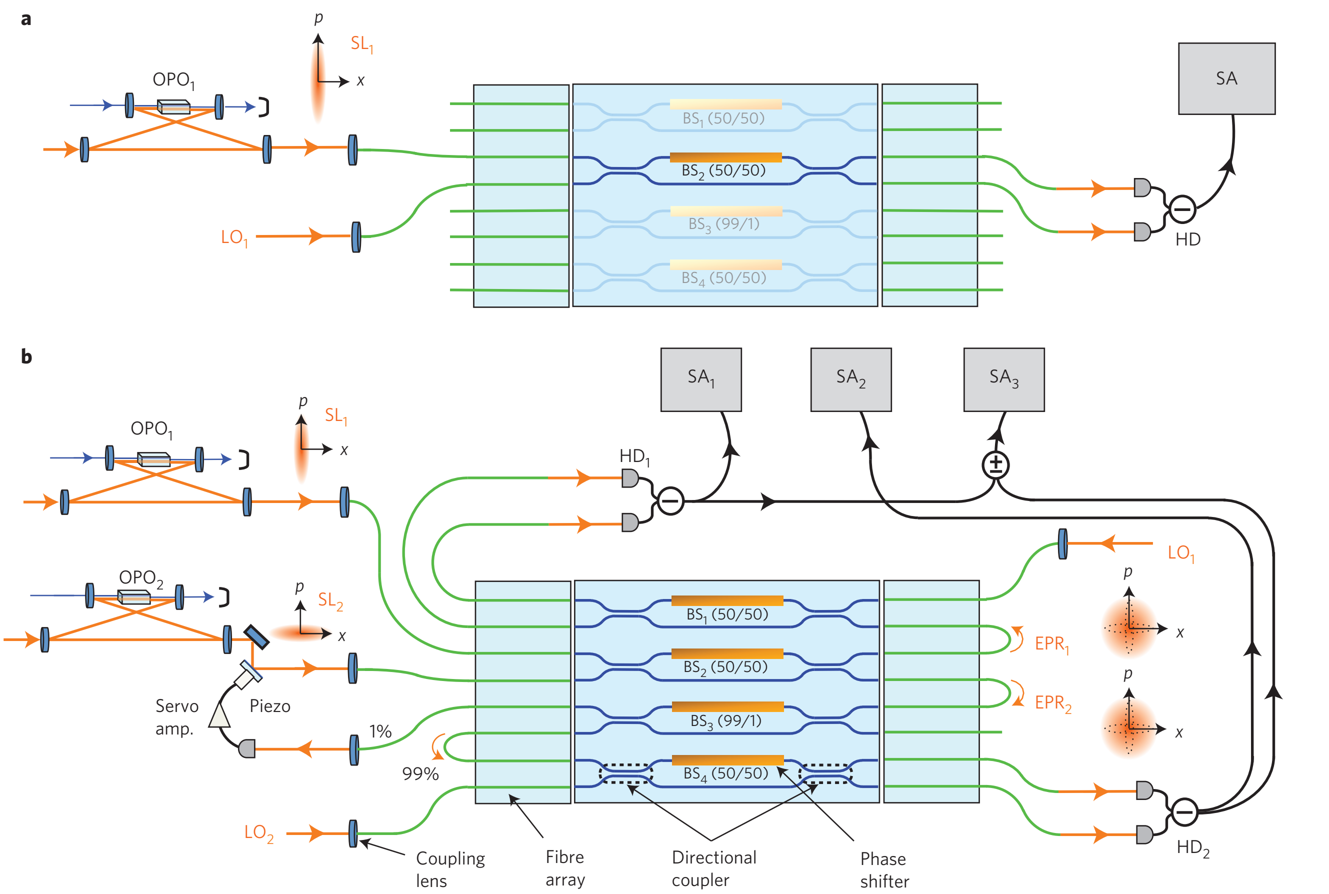

Figure 1 | Experimental set-up. Four variable-reflectivity beamsplitters are implemented in a photonic chip. Each variable beamsplitter is composed of two directional couplers and a variable phase shifter. Beamsplitters BS$_1$, BS$_2$ and BS$_4$ are tuned at a splitting ratio of 50/50 and BS$_3$ at 99/1. A pair of fibre arrays are used for both entrance and exit facets of the chip to inject and eject beams efficiently. To guide the output from one beamsplitter to another, two fibres are connected mechanically. Continuous-wave squeezed lights SL$_1$ and SL$_2$ (at 860 nm) are generated by sub-threshold optical parametric oscillators (OPOs)[25,26] outside the chip. A pump beam at 430 nm for the OPOs is generated by an optical frequency doubler[27]. Weak coherent beams are introduced into both OPOs for the purpose of phase-locking. **a**, Balanced homodyne measurement of squeezed light within the chip. Squeezed light SL$_1$ is combined with local oscillator LO$_1$ and detected by a balanced homodyne detector (HD) outside the chip. **b**, Generation and characterization of EPR beams within the chip. Two squeezed lights SL$_1$ and SL$_2$ are first combined at BS$_2$. One percent of the weak coherent beams is picked up by BS$_3$ and used for phase-locking between squeezed lights SL$_1$ and SL$_2$ at 90° using a servo-amplifier and piezo actuator. Output beam EPR$_1$ (EPR$_2$) is combined with local oscillator LO$_1$ (LO$_2$) at BS$_1$ (BS$_4$) and then detected by balanced homodyne detector HD$_1$ (HD$_2$).

Figure 2a presents typical results for homodyne measurement of squeezed light SL$_1$, which was generated by using a sub-threshold optical parametric oscillator (OPO) with a pump power of 100 mW. As the LO phase is varied using a piezoelectric controller, the observed signal oscillates between a squeezing level of -4.02 ± 0.13 dB and an anti-squeezing level of $+11.85 \pm 0.15$ dB. The measurement was repeated for different pump powers. Figure 2b shows the squeezing and anti-squeezing levels as the pump power is varied. The solid curves show calculation results (Supplementary Section II) with almost perfect visibility (0.995) and show good agreement with the experimental values. Saturation of the squeezing level at about -4 dB at a higher pump power is predominantly due to an insufficient overall coupling efficiency (0.72), consistent with the -8.4 dB of squeezing level expected for a perfect coupling efficiency. These results and their agreement with calculations demonstrate the high performances of our integrated device for CV operation. In particular, a high degree of mode matching (interference between two coherent beams shows visibilities of 0.995) and low levels of stray light noise (as a result of the side band measurement) enable the transmission and detection of high levels of squeezing.

We now describe the central result of this work: the generation and characterization of EPR beams within the chip. To characterize the amount of entanglement obtained with our system we use an inseparability criterion. If we introduce the quadrature phase amplitude operators $\hat{x}$ and $\hat{p}$, which correspond to cosine and sine components of the optical field, we can write the complex amplitude operators of output modes EPR$_1$ and EPR$_2$ as $\hat{a}_1 = \hat{x}_1 + i\hat{p}_1$ and $\hat{a}_2 = \hat{x}_2 + i\hat{p}_2$, respectively. To evaluate the entanglement between two output beams, we define the correlation variance $\Delta^2_{1,2}$ as

$$\Delta^2_{1,2} = \langle [\Delta(\hat{x}_1 - \hat{x}_2)]^2 \rangle + \langle [\Delta(\hat{p}_1 + \hat{p}_2)]^2 \rangle. \tag{1}$$

It has been proven by Duan and colleagues[17] and Simon[18] that two beams are inseparable when $\Delta^2_{1,2} < 1$, demonstrating entanglement. It is also possible to re-write $\Delta^2_{1,2}$ as a function of the squeezing parameter r of the input beams, and in this case we have $\Delta^2_{1,2} = e^{-2r}$. It can easily be seen that $\Delta^2_{1,2}$ goes to zero in the ideal case with an infinite amount of squeezing, achieving perfect correlation.

Experimentally, we generate the EPR beams by combining two squeezed lights SL$_1$ and SL$_2$ at beamsplitter BS$_2$ and locking the relative phase between them, $\theta_{1,2}$, at 90° (Fig. 1b)[4]. Quantum

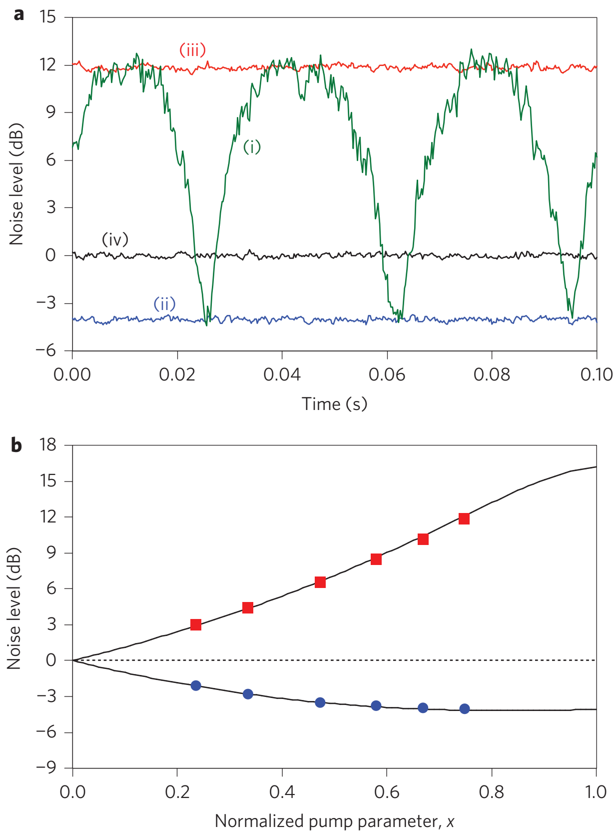

Figure 2 | On-chip homodyne detection of squeezing. a, Quantum noise level of squeezed light generated with a pump power of 100 mW. Trace (i): LO phase is scanned. Trace (ii): LO phase is locked at the squeezed quadrature. Trace (iii): LO phase is locked at the anti-squeezed quadrature. Trace (iv): the shot noise level is normalized to 0 dB. Resolution bandwidth, 30 kHz. Video bandwidth, 300 Hz. Traces (ii), (iii) and (iv) are averaged 20 times. **b**, Pump power dependence of the squeezing and anti-squeezing levels. The normalized pump power x is defined as $\sqrt{(P/P_{\mathrm{th}})}$, where $P_{\mathrm{th}} = 179$ mW is the oscillation threshold of the OPO. Circles and squares indicate observed squeezing and anti-squeezing levels, respectively, and solid curves show the results of numerical calculations.

entanglement is verified with a homodyne measurement, using beamsplitters BS_1 and BS_4 to combine the two EPR beams with two LO beams. In this case the experiment is also performed at the 1.5 MHz side band of the laser frequency. Figure 3a and b show the noise levels of output beams EPR_1 and EPR_2, respectively, as the phase of the LO is varied. Trace (i) represents the noise of one of the output beams as $\theta_{1,2}$ is varied while simultaneously scanning the LO phase on a faster timescale. The outputs continuously tune from EPR beams to two independent squeezed light beams as $\theta_{1,2}$ changes from 90 to 0° (ref. 19). Traces (ii) and (iii) represent the noise levels of the x and p quadratures when $\theta_{1,2}$ is locked at 90°. We observed noise levels of $\langle \Delta\hat{x}_1^2\rangle = +4.91 \pm 0.13$ dB and $\langle \Delta\hat{p}_1^2\rangle = +4.85 \pm 0.15$ dB for output EPR_1 at HD_1 and $\langle \Delta\hat{x}_2^2\rangle + 4.10 \pm 0.12$ dB and $\langle \Delta\hat{p}_2^2\rangle = +4.18 \pm 0.13$ dB for output EPR_2 beam at HD_2, above the shot noise level represented by trace (iv). This phase-insensitive behaviour is one of the essential properties of EPR beams: entangled states show strong correlations with each other, but the individual properties are not well defined (tracing out either beam of a maximally entangled state leaves the other beam in a maximally mixed state).

Finally, we measured $\langle [\Delta(\hat{x}_1 - \hat{x}_2)]^2\rangle$ and $\langle [\Delta(\hat{p}_1 + \hat{p}_2)]^2\rangle$ to check the inseparability criterion. Trace (i) in Fig. 3c shows the variance of the difference signal between $\hat{x}_1$ from HD_1 and $\hat{x}_2$ from HD_2, which are taken using a hybrid junction. Trace (ii) represents the variance of the sum signal between $\hat{p}_1$ and $\hat{p}_2$ obtained in the same way. We achieve $\langle [\Delta(\hat{x}_1 - \hat{x}_2)]^2\rangle = -1.44 \pm 0.12$ dB and $\langle [\Delta(\hat{p}_1 + \hat{p}_2)]^2\rangle = -1.49 \pm 0.12$ dB below the noise level without quantum correlation, as shown by trace (iii). These results yield a correlation variance of $\Delta_{1,2}^2 = 0.71$ and satisfy the inseparability criterion, proving the generation of EPR beams and characterization of quantum entanglement within our photonic chip.

Our demonstration of all the key components for Gaussian operations within a photonic chip, including the generation and characterization of EPR beams and the verification of entanglement, points the way to full optical integration of CV and hybrid quantum information processing. The use of side bands of the optical field (to circumvent noise caused by stray light), combined with high-quality interference due to perfect mode-matching in directional couplers, enables simultaneous operation on non-classical light and intense coherent beams in a single photonic chip. Coupling in and out of the device is the major contributor to loss, which limits entanglement. This can be dramatically reduced by concatenating circuits

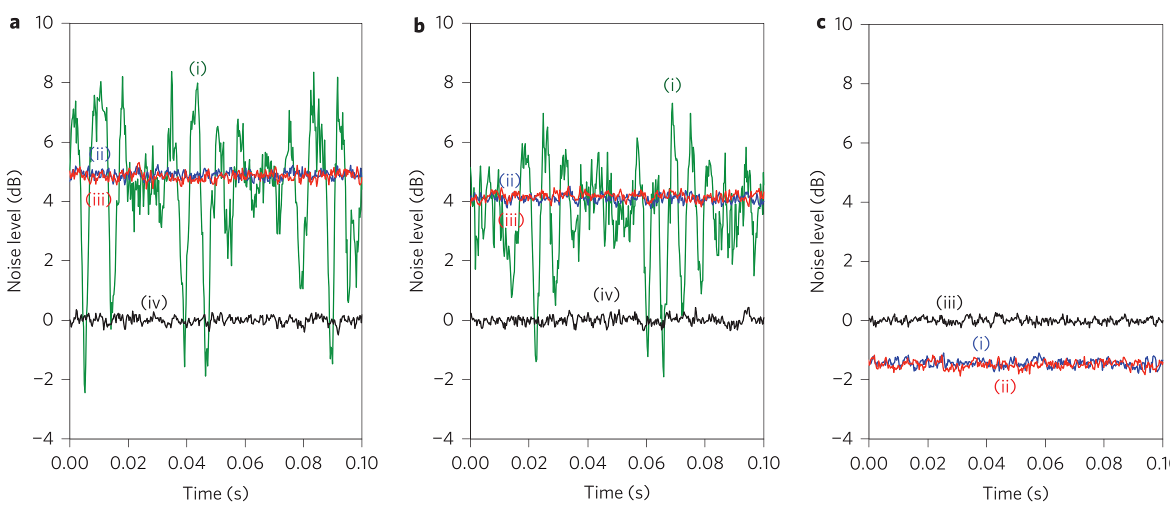

Figure 3 | EPR entanglement verification. a,**b**, Noise levels for output beam EPR_1 (**a**, trace (i)) and output beams EPR_2 (**b**, trace (i)), where $\theta_{1,2}$ is changed and the LO phase is simultaneously scanned with a faster timescale. Traces (ii) and (iii): noise levels where the LO phase is locked at the x and p quadrature with the $\theta_{1,2}$ locked at 90°. Trace (iv): shot noise level normalized to 0 dB. **c**, Inseparability condition measurement. Traces (i) and (ii) represent $\langle [\Delta(\hat{x}_1 - \hat{x}_2)]^2\rangle$ and $\langle [\Delta(\hat{p}_1 + \hat{p}_2)]^2\rangle$, respectively, and trace (iii) shows the noise level without quantum correlation.

in a single integrated network. Further performance gains will be achieved by the integration of photodiodes on the photonic chip, as has been achieved with waveguide-coupled single-photon detectors[20,21], further removing the requirement for coupling out from the chip to fibres. Universal quantum information processing will require non-Gaussian operations like photon counting[22]. Integrated semiconductor[23] or superconducting[21] detectors are promising, and will enable the use of side-band techniques using the recently developed optical high-pass filter[24], thereby eliminating the influence of stray light that would affect the detection of dark counts.

Received 22 October 2014; accepted 20 February 2015; published online 30 March 2015

References

1. O'Brien, J. L., Furusawa, A. & Vučković, J. Optical quantum computing. *Nature Photon.* **3,** 687–695 (2009).
2. Einstein, A., Podolsky, B. & Rosen, N. Can quantum-mechanical description of physical reality be considered complete? *Phys. Rev.* **47,** 777–780 (1935).
3. Braunstein, L. & van Loock, P. Quantum information with continuous variables. *Rev. Mod. Phys* **77,** 513–577 (2005).
4. Furusawa, A. & van Loock, P. *Quantum Teleportation and Entanglement: A Hybrid Approach to Optical Quantum Information Processing* (Wiley-VCH Verlag, 2011).
5. Dowling, J. P. & Milburn, G. J. Quantum technology: the second quantum revolution. *Phil. Trans. R. Soc. Lond. A* **361,** 1655–1674 (2003).
6. Bouwmeester, D. *et al.* Experimental quantum teleportation. *Nature* **390,** 575–579 (1997).
7. O'Brien, J. L. Optical quantum computing. *Science* **318,** 1567–1570 (2007).
8. Furusawa, A. *et al.* Unconditional quantum teleportation. *Science* **282,** 706–709 (1998).
9. Weedbrook, C. *et al.* Gaussian quantum information. *Rev. Mod. Phys.* **84,** 621–669 (2012).
10. Jeong, H. *et al.* Generation of hybrid entanglement of light. *Nature Photon.* **8,** 564–569 (2014).
11. Morin, O. *et al.* Remote creation of hybrid entanglement between particle-like and wave-like optical qubits. *Nature Photon.* **8,** 570–574 (2014).
12. Takeda, S. *et al.* Deterministic quantum teleportation of photonic quantum bits by a hybrid technique. *Nature* **500,** 315–318 (2013).
13. Politi, A., Cryan, M. J., Rarity, J. G., Yu, S. & O'Brien, J. L. Silica-on-silicon waveguide quantum circuits. *Science* **320,** 646–649 (2008).
14. Matthews, J. C. M., Politi, A., Stefanov, A. & O'Brien, J. L. Manipulation of multiphoton entanglement in waveguide quantum circuits. *Nature Photon.* **3,** 346–350 (2009).
15. Shadbolt, P. J. *et al.* Generating, manipulating and measuring entanglement and mixture with a reconfigurable photonic circuit. *Nature Photon.* **6,** 45–49 (2012).
16. Laing, A. *et al.* High-fidelity operation of quantum photonic circuits. *Appl. Phys. Lett.* **97,** 211109 (2010).
17. Duan, L.-M., Giedke, G., Cirac, J. I. & Zoller, P. Inseparability criterion for continuous variable systems. *Phys. Rev. Lett.* **84,** 2722–2725 (2000).
18. Simon, R. Peres–Horodecki separability criterion for continuous variable systems. *Phys. Rev. Lett.* **84,** 2726–2729 (2000).
19. Zhang, T. C., Goh, K. W., Chou, C. W., Lodahl, P. & Kimble, H. J. Quantum teleportation of light field. *Phys. Rev. A* **67,** 033802 (2003).
20. Sprengers, J. P. *et al.* Waveguide superconducting single-photon detectors for integrated quantum photonic circuits. *Appl. Phys. Lett.* **99,** 181110 (2011).
21. Pernice, W. H. P. *et al.* High-speed and high-efficiency travelling wave single-photon detectors embedded in nanophotonic circuits. *Nature Commun.* **3,** 1325 (2012).
22. Dakna, M., Anhut, T., Opatrný, T., Knöll, L. & Welsch, D.-G. Generating Schrödinger-cat-like states by means of conditional measurements on a beam splitter. *Phys. Rev. A* **55,** 3184–3194 (1997).
23. Campbell, J. C. Recent advances in telecommunications avalanche photodiodes. *J. Lightw. Technol.* **25,** 109–121 (2007).
24. Takeda, S. *et al.* Quantum mode filtering of non-Gaussian states for teleportation-based quantum information processing. *Phys. Rev. A* **85,** 053824 (2012).
25. Suzuki, S., Yonezawa, H., Kannari, F., Sasaki, M. & Furusawa, A. 7 dB quadrature squeezing at 860 nm with periodically poled $KTiOPO_4$. *Appl. Phys. Lett.* **89,** 061116 (2006).
26. Takeno, Y., Yukawa, M., Yonezawa, H. & Furusawa, A. Observation of −9 dB quadrature squeezing with improvement of phase stability in homodyne measurement. *Opt. Express* **15,** 4321–7327 (2007).
27. Masada, G. *et al.* Efficient generation of highly squeezed light with periodically poled $MgO{:}LiNbO_3$. *Opt. Express* **18,** 13114–13121 (2010).

Acknowledgements

The authors thank H. Bachor for advice. This work was partly supported by the Project for Developing Innovation Systems (PDIS), Grants-in-Aid for Scientific Research (GIA) and the Advanced Photon Science Alliance (APSA) commissioned by the Ministry of Education, Culture, Sports, Science and Technology (MEXT) of Japan, the Nippon Telegraph and Telephone Corporation (NTT), the Engineering and Physical Sciences Research Council (EPSRC), the European Research Council (ERC), Photonic Integrated Compound Quantum Encoding (PICQUE), Breaking the Barriers of Optical Integration (BBOI), the US Army Research Office (ARO; grant no. W911NF-14-1-0133) and the US Air Force Office of Scientific Research (AFOSR). J.L.O. acknowledges a Royal Society Wolfson Merit Award and a Royal Academy of Engineering Chair in Emerging Technologies.

Author contributions

A.F. and J.L.O. planned the project. A.F. supervised the project. G.M. and K.M. conducted the experiment and data analysis. J.L.O. and A.P. developed the waveguide chip. T.H. provided experimental information. G.M., A.P., J.L.O. and A.F. wrote the manuscript with assistance from T.H. and K.M.

Additional information

Supplementary information is available in the online version of the paper. Reprints and permissions information is available online at www.nature.com/reprints. Correspondence and requests for materials should be addressed to A.F.

Competing financial interests

The authors declare no competing financial interests.